Applied Composite Materials (2024) 31:489–509
https://doi.org/10.1007/s10443-023-10181-1

Crashworthiness of Foam-Filled and Reinforced Honeycomb Crash Absorbers in Transverse Direction

G. Nicoud[1] · H. Ghasemnejad[1] · S. Srimanosaowapak[2] · J. W. Watson[3]

Received: 26 July 2023 / Accepted: 13 November 2023 / Published online: 29 November 2023

Abstract
Honeycomb crash absorbers have been widely studied as energy absorption devices for use in automotive industries. However, none of these investigations have studied the side impact of empty and foam-filled honeycomb absorbers and adding stiffeners between the different layers of the corrugated sheets which are composing the honeycomb structure to analyse the structure under transverse (L-direction) impacts. In this paper, the foam-filled and reinforced honeycomb crash absorbers are investigated under axial (T) and transverse (L) loading directions. Experimental results for both empty and foam-filled specimens under quasi-static and impact loads were implemented to validate the developed finite element model. Finite element analysis (FEA) was performed to find out the crashworthiness behaviour of the structure under axial and transverse impacts according to road conditions. Finally, a new design of stiffened honeycomb crash absorber was developed and investigated to reduce the level of acceleration experienced by the passengers during the crash event. In this regard, it is concluded that all the requirements related to the energy absorption capabilities and generated deceleration under impact loading can be met by introducing an advanced method to reinforce honeycomb absorbers using stiffeners. It is also proven that the thickness of these stiffeners will not significantly influence the force levels. Due to increase of wall thickness from 1 to 3 mm, the mean crushing force increased from 129 kN to 148 kN. This growth is not sufficient as the goal is to obtain a mean crushing force of 300 kN. Thickening the stiffeners would lead to a loss of efficiency of the structure, as the small increase in mean force would not make up for the gain in mass. Thus, increasing the corrugated sheet' thickness becomes necessary.

Keywords Aluminium honeycomb · Aluminium foam · Foam-filled structures · Stiffeners

✉ H. Ghasemnejad
Hessam.Ghasemnejad@cranfield.ac.uk

[1] School of Aerospace, Transport and Manufacturing (SATM), Cranfield University, MK430AL Cranfield, UK

[2] National Metal and Materials Technology Center (MTEC), Pathum Thani 12120, Thailand

[3] Cranfield Impact Centre (CIC), Cranfield MK43 0AL, UK

1 Introduction

Accidents that occur during road construction and maintenance frequently result in worker fatalities and injuries. Vehicles that unintentionally enter the work zone are one of the causes. The statistics show how the development of safer working circumstances, such as better work training in regulated work zones, the use of traffic control devices, and protective gear, and the imposition of stronger law enforcement on drivers, led to a drop in the number of accidents. This condition calls for the use of protective equipment that is readily available because it can prevent accidents for workers and lessen the severity of accidents for drivers. According to related research, the honeycomb structure has a high strength which can absorb a significant amount of impact energy. This research aims to create a workpiece that can mitigate the fatality and injury of road accidents on the expressway by improving the crashworthiness performance of the crash box of a road service vehicle. The primary goal of this crash box is indeed to deflect impact energy to protect work zone accessibility and lessen the severity of accidents. It is a key element of impact force severity reduction technology that can be mounted at various locations on both stationary and mobile objects. Further research will be done on the design and construction of the entire workpiece. The specific energy absorption is the primary factor which is used to assess how an energy-absorbing device would behave and evaluate the crashworthiness performance. This characteristic determines the quantity of energy absorbed and enables comparison with structures that are comparable but have a different mass. As a result, it is possible to test various combinations of foam-filled cells to determine which structure performs best given a certain energy absorption requirement.

Additionally, it is important to keep the maximum forces under control, which are directly linked to the maximum acceleration levels. Humans can only tolerate a limited level of deceleration during an impact, which is the reason why one of the major design criteria is set not to exceed this deceleration threshold. In this regard, foam-filled structures play a significant role since the number of aluminium foams functions as a limiter for the maximum force. Partovi Meran et al. [1] conducted a numerical and experimental study to determine the effects of various honeycomb design parameters, such as honeycomb cell thickness, side size, and cell expansion angle, on the resistance to out-of-plane impact. Specific energy absorption (SEA) and crush force efficiency (CFE), two crashworthiness parameters, are dependent on these parameter changes. The energy absorption capability increases as cell thickness increases or, on the contrary, as cell size decreases. Wierzbicki [2] studied the mean crushing stress and pressure of hexagonal honeycomb structures. He determined a new method for predicting the mean crushing stress of honeycomb structures with various cell specifications under axial loading, based on the Super Folding Element theory. It can be determined with the value of the flow stress, cell wall thickness and width of the cell wall. When it comes to the mean crushing pressure in the axial direction, Wierzbicki found out that it depends once again on the flow stress and the so-called relative cell thickness. Increases in the mean crushing pressure could, then, be attributed to different flow stress under dynamic loading. Garai et al. [3] investigated different filling methods as foam-filling appears to be a better solution than using thicker tubes to absorb the same energy with less weight. He examined three different filling methods of the aluminium foam pieces by bending and compression tests, joining with heat dilatation, pressing and adhesive bonding.

Dipen Kumar Rajak et al. [4] observed the increase in the crash load efficiency and specific energy absorption between empty and foam-filled tubes, by a factor of 1.56 for the energy absorption of aluminium foam-filled mild steel single tubes as compared to empty ones. Similarly, Hsu and Jones [5] concluded that the effects of foam-filling in single tubes are an increase in the average crushing load over that of the tube and foam alone: this phenomenon is called the interaction effect, and a decrease in the fold length. Furthermore, they studied the effect of multiple tube packing which increased crushing and average crushing load values over the sum of the average crushing loads of the equal number of single empty and foam-filled tubes. The increase in the average crushing loads of multi-tube designs over the single tubes was attributed to the constraint effects and frictional forces between tubes and tubes and outer tube walls. Another way to improve the crashworthiness behaviour of honeycomb structures even further is to add a stiffener between each corrugated sheet. He and Ma [6] studied the deformation performance of these reinforced hexagonal honeycombs. It was concluded that peak stress increases with stiffener thickness and expanding angle has no adverse effect on the peak stress of the reinforced hexagonal honeycomb. However, the impact velocity appears to have a significant effect on the mean crushing stress and the primary peak stress due to the existence of the lateral inertia effect. Finally, the main conclusion was that, compared to the traditional regular hexagonal honeycomb, the reinforced regular hexagonal honeycomb has a better energy absorption performance under the same limit of peak stress.

Various investigations have been performed on the effect of crashworthiness of polymeric composite tubular elements [7–20]. The authors have performed experimental and numerical studies to investigate the effect of HNC, MC, Al_2O_3, SiO_2, and SiC nanofillers on the specific energy absorption (SEA) and crush force efficiency (CFE) of GFPR composite elements.

However, none of these investigations have studied the side impact of empty and foam-filled honeycomb absorbers and adding stiffeners between the different layers of the corrugated sheets which are composing the honeycomb structure in order to analyse the structure under transverse (L-direction) impacts. In this regard, the effect of stiffeners on the energy absorption capability of crash boxes is considered as the main novelty of this research. In this research paper, the design of honeycomb structures will be improved and compared with the performance in axial impacts. In the end, the structure should be able to absorb the energy of a 1500 kg car crashing at 50 km/h into it, without compromising the life of the passengers by causing excessive levels of deceleration.

2 Experimental Tests

Experimental tests were conducted to confirm the validity of the finite element models. As a result, four quasi-static impact tests and four dynamic impact tests were conducted at the Cranfield Impact Centre (CIC), including testing of both empty and foam-filled structures, as well as testing in both the axial (T) and side (L) directions.

Depending on the orientation of the honeycomb structure, two types of side impact tests could be conducted, as shown in Fig. 1. Due to the weakness of specimens in the W-direction (welded joints) and manufacturer recommendations, the L-direction has been considered in this work only.

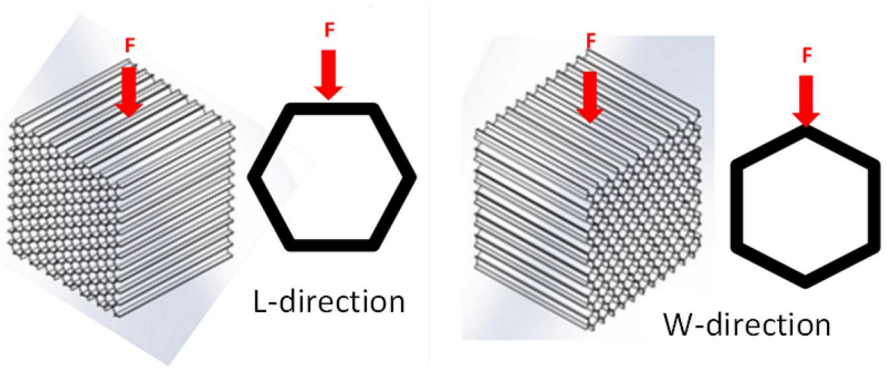

Fig. 1 Comparison between side impact test in L-direction and W-direction (left to right)

2.1 Material Properties

2.1.1 Aluminium Honeycomb

Honeycomb structures were made of 1100 aluminium alloy in the H14 temper (Al-0.95 Si + Fe-0.2 Cu-0.1 Zn-0.05 Mn (wt%)) using a corrugated process. Sheets were folded and stacked into blocks whose corrugated nodes and outside flat sections of the corrugated sheets were welded. Tensile tests were performed at the Thailand National Metal and Materials Technology Centre to obtain the material properties of the aluminium used for the corrugated sheets. The results of these tests were presented in [21]. Young's modulus and Poisson's ratio were extracted from these tests. The average values of Young's modulus and Poisson's ratio obtained from the five tensile tests are 57.25 GPa and 0.33, respectively.

2.1.2 Aluminium Foam

Open-cell aluminium foam fillers with hybrid pore sizes of 2 and 16 mm were made of A356.2 alloy with T6 heat treatment using a vacuum infiltration technique. Modelling the compressive behaviour of the aluminium foam fillers is achieved through the compressive tests, using a crosshead speed of 18 mm/min, conducted at the Thailand National Metal and Materials Technology Centre. These tests are performed under the standard BS ISO 13314:2011 – Ductility testing – Compression test for porous and cellular metals [22].

Several compression tests had already been performed for different foam densities from 860 to 970 kg/m^3 and were presented in [21]. However, it was established that the optimum foam density was around 400 kg/m^3. Aluminium foams with a density of around 400 kg/m^3 were tested and the properties of the specimen are given in Table 1. The shape of the specimens is hexagonal to match the shape of the foam fillers.

The stress-strain curve of the five specimens tested under compression is shown in Fig. 2. The behaviour of the open-cell foams shows the succession of an elastic region, a plateau region, and a densification zone. These different parameters can define the foam material model.

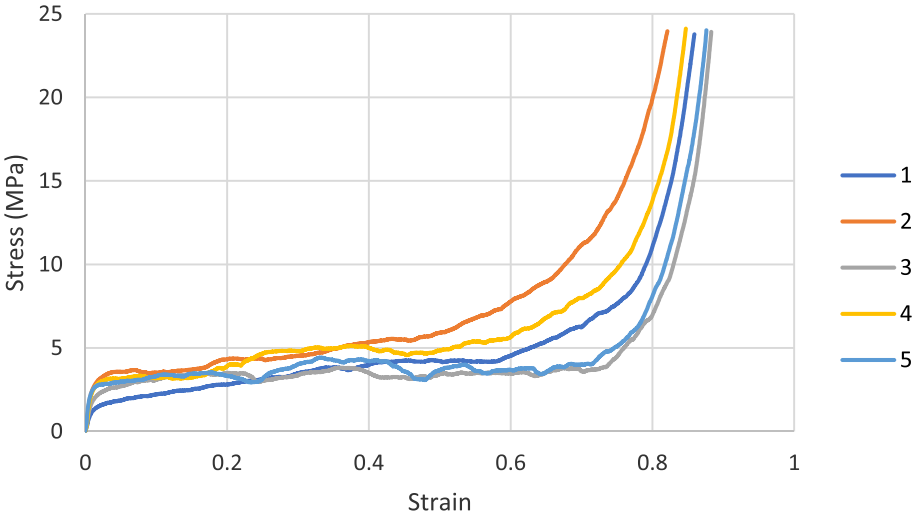

Fig. 2 Stress-strain curve of the compression tests for the different specimens

2.2 Honeycomb Specimens

Four quasi-static and four dynamic tests were performed, implying the use of eight different specimens, four of which are empty specimens and four of which are foam-filled specimens. For the foam-filled specimens, aluminium foams were filled into the honeycomb cells without bonding. The top view of the two types of specimens is represented in Fig. 4.

The overview of these different test conditions and dimensions of the testing specimen is given in Fig. 3. The dimensions of the honeycomb specimens are shown in Table 2.

2.3 Quasi-static Experimental Tests

2.3.1 T-direction

Quasi-static tests are performed to measure the mean crushing force of the different specimens, and most importantly the energy absorption capability of the structure. The quasi-static test performed is a compression test at a speed rate of 2 mm/min. The honeycomb structure is crushed between a plate and either a half-moon-shaped impactor or another plate, depending on the direction of the impact test. The setup for both T-direction and L-direction quasi-static tests is shown in Fig. 5.

Table 1 Properties and dimensions of aluminium foam specimens

Specimen No.	1	2	3	4	5
Density (kg/m^3)	0.40	0.43	0.41	0.40	0.39
Porosity (%)	85.15	83.92	84.49	85.14	85.29
Height (mm)	100.30	100.20	100.20	100.30	100.30
Mass (g)	66.78	71.68	69.35	65.80	65.34

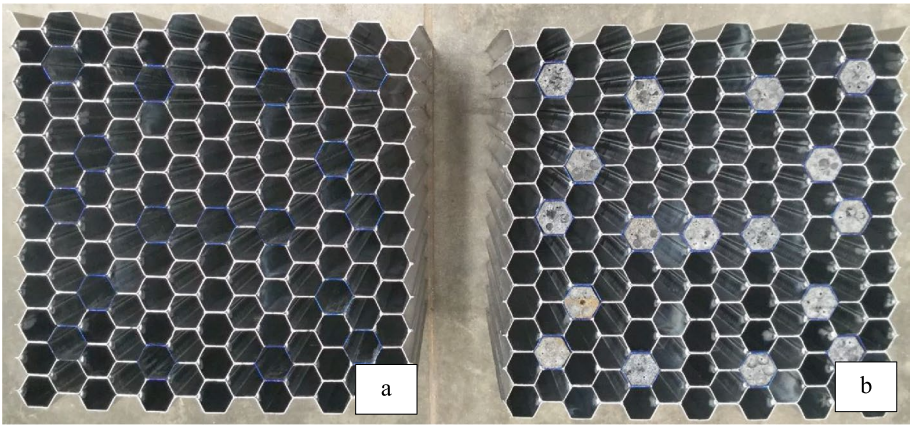

Fig. 3 Description of the testing conditions in T-directions

Two T-direction quasi-static tests were performed, one on the empty honeycomb specimen, and the other on the foam-filled honeycomb specimen. Figure 6 indicates the comparison of the force-displacement curves from these two tests, along with a table containing the most relevant parameters allowing to predict of the structural behaviour during an impact, and also allowing to determine the maximum energy input which can be given to the trolley during the dynamic impact tests.

2.3.2 L-direction

The L-direction quasi-static tests were also performed, one on the empty honeycomb specimen, and the other on the foam-filled honeycomb specimen. Figure 7 shows the comparison

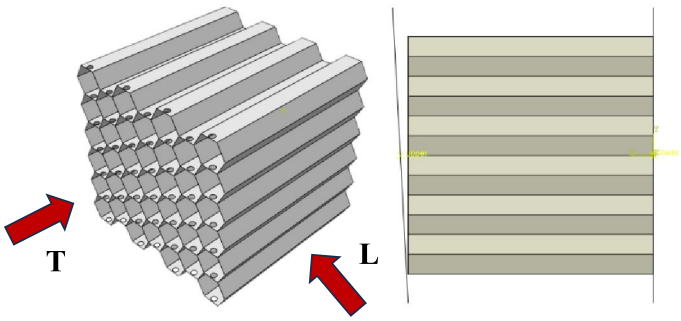

Load direction	T		T		L		L	
Honeycomb	Empty	Foam-filled	Empty	Foam-filled	Empty	Foam-filled	Empty	Foam-filled
Test condition	Dynamic	Dynamic	Static	Static	Dynamic	Dynamic	Static	Static
Specimen No.	1	2	3	4	5	6	7	8
Mass (kg)	19.6	25.0	19.5	24.9	19.6	24.9	19.5	25.0

Fig. 4 Top view of (**a**) empty and (**b**) foam-filled specimens

Table 2 Dimensions of honeycomb specimens

Honeycomb Geometry	Dimensions
Width (mm)	484
Length (mm)	442
Height (mm)	500
Single thickness (mm)	1
Double thickness (mm)	2
Cell height (mm)	47.2
Cell width (mm)	40.2

of the force-displacement curves from these two tests, along with a table containing the most relevant parameters. The tests were stopped for an end displacement of 0.3 m, as both structures enter the densification zone, which means the structure reached its full potential and can no longer deform to absorb any further energy. The deformed structures after the L-direction quasi-static tests are shown in Fig. 8.

2.4 Impact Tests

Following the quasi-static tests, the impact tests were conducted using the same impactor shapes for each type of test, T-direction or L-direction. The impact tests are crucial for assessing how the structure behaves under the conditions of a real road accident.

2.4.1 T-direction Impact Tests

The T-direction impact tests were performed following the same pattern as for the quasi-static tests: one on the empty honeycomb specimen, and the other on the foam-filled honeycomb specimen. Figures 9 and 10 shows the comparison of the force-displacement curves from these two tests, along with a table containing the most relevant parameters allowing us to understand the structural behaviour during the impact.

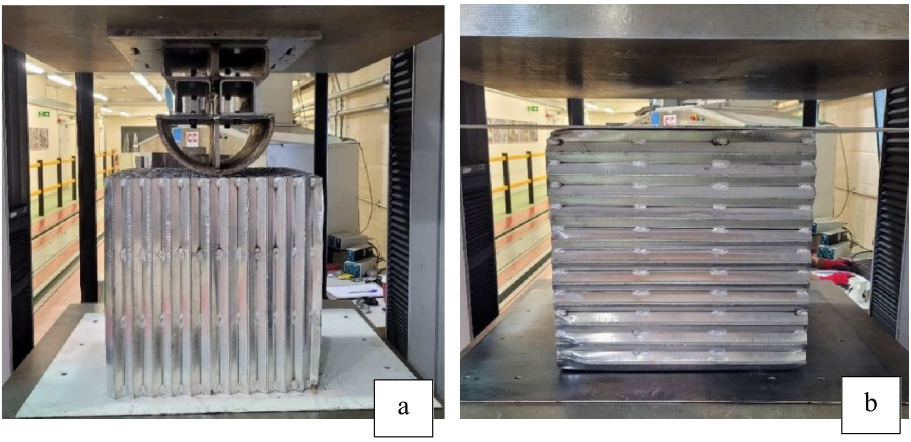

Fig. 5 Quasi-static (**a**) axial and (**b**) side compression tests on honeycomb specimens

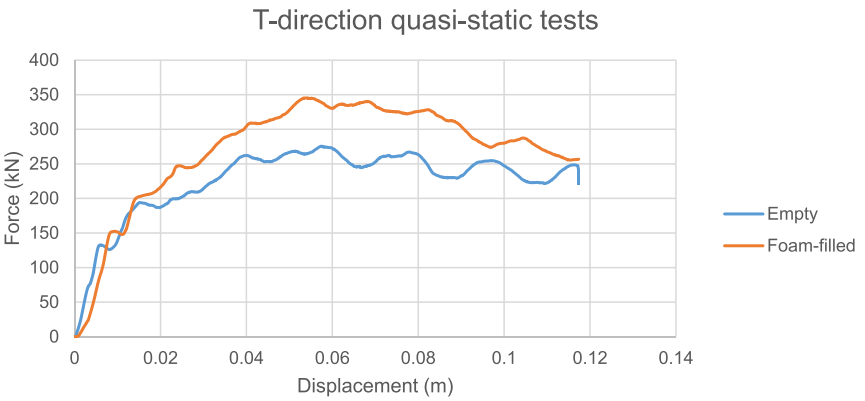

	Empty	Foam-filled
Peak force (kN)	276±2	345±2
Mean crushing force (kN)	226±2	270±2
EA (kJ)	26.5±1	31.8±1
Mass (kg)	19.5±1	24.9±1
SEA (kJ/kg)	1.36±0.5	1.27±0.2

Fig. 6 T-direction quasi-static force-displacement graphs and results, (average of test data for 3 specimens in each case)

First, it can be noticed that the energy absorption of both structures is the same, even though the two force-displacement curves do not look the same. The slight difference in the energy absorption value is only due to the slight difference in the velocity of the impactor between both tests.

Furthermore, the curves indicate that the end displacement of the foam-filled specimen is widely lower than for the empty specimen; the foam-filled specimen can absorb all the impact energy within approximately 0.2 m against 0.25 m, a reduction of 20% against the empty specimen. On the other hand, the peak force for the foam-filled specimen is greater, which means that the acceleration level is also greater.

Considering the SEA values, one can only conclude that for these precise test conditions, the empty specimen is more interesting from a crashworthiness perspective than the foam-filled specimen. However, suppose the velocity and mass of the impactor were increased. In that case, it may be possible that the foam-filled specimen became more attractive as the full potential of the foam-filled structure would be approached (see Fig. 11).

2.4.2 L-Direction Impact Tests

The L-direction impact tests were also performed following the same pattern as for the quasi-static tests: one on the empty honeycomb specimen, and the other on the foam-filled honeycomb specimen. Figure 12 shows the comparison of the force-displacement curves from these two tests, along with a table containing the most relevant parameters allowing us to understand the structural behaviour during the impact.

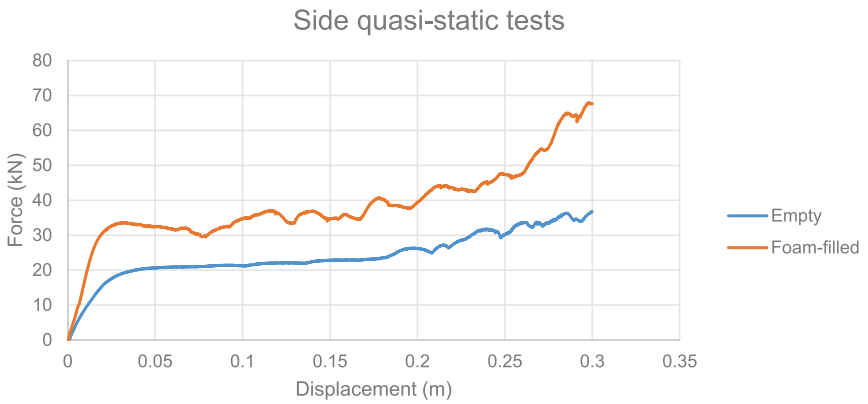

	Empty	Foam-filled
Peak force (kN)	37±2	68±2
Mean crushing force (kN)	24±1	39±2
EA (kJ)	7.2±2	11.6±1
Mass (kg)	19.5±1	25.0±2
SEA (kJ/kg)	0.37±2	0.46±1

Fig. 7 Side quasi-static force-displacement curves and results (average of test data for 3 specimens in each case)

As for the T-direction tests, it can also be noticed that the energy absorption of both structures is the same for both structures. This is because both structures can absorb all the kinetic energy provided by the impactor.

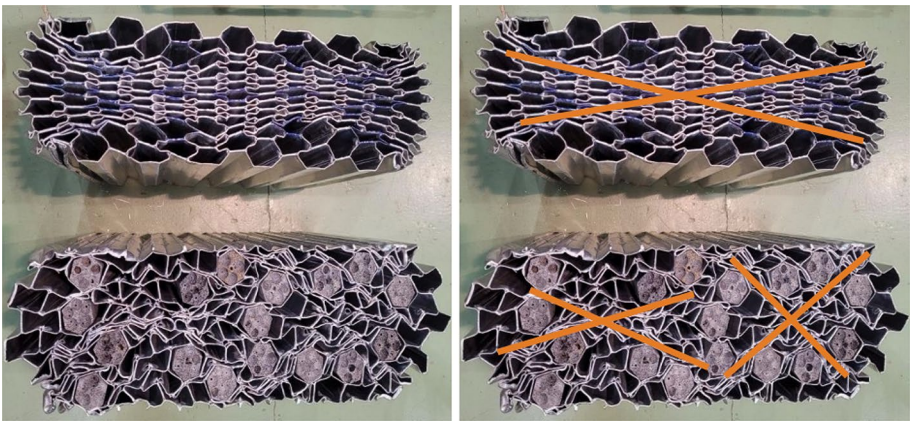

Fig. 8 Top view and deformation pattern of empty and foam-filled specimens after the L-direction quasi-static tests

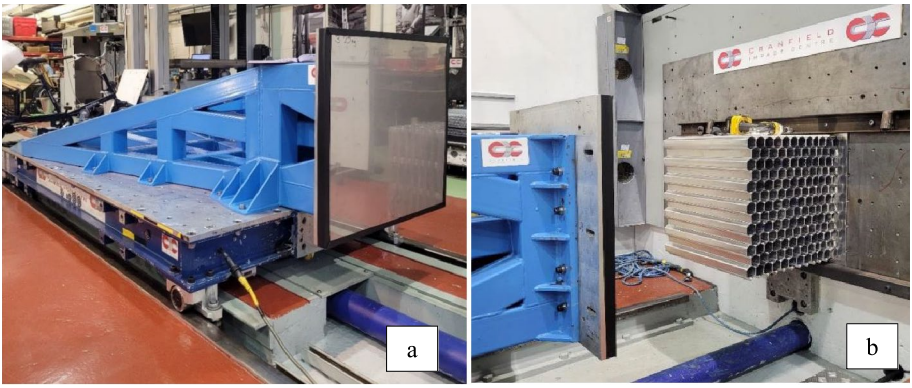

Fig. 9 Impact test trolley at Cranfield Impact Centre (CIC), (**a**) impactor and (**b**) test setup

Moreover, the curves indicate that the end displacement of the foam-filled specimen is significantly lower than for the empty specimen; the foam-filled specimen can absorb all the impact energy within approximately 0.24 m against close to 0.28 m, being a reduction of 16% against the empty specimen. On the other hand, the peak force for the foam-filled specimen

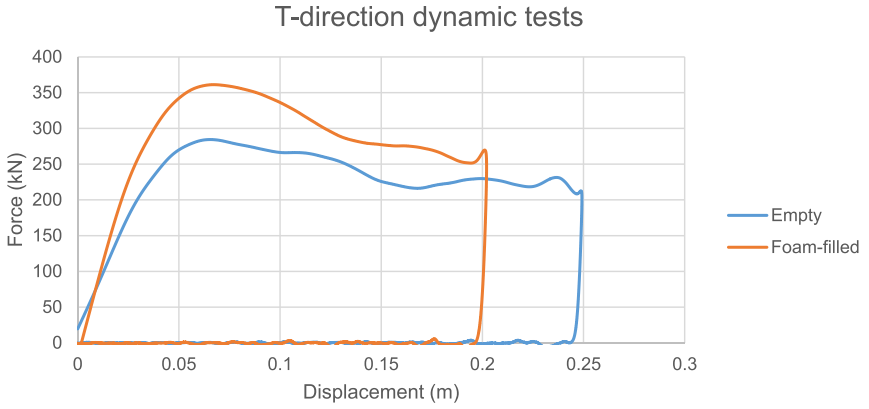

	Empty	Foam-filled
Peak force (kN)	284±2	361±2
Mean acceleration (g)	25±2	31±1
Displacement (m)	0.249±0.02	0.202±0.02
EA (kJ)	56.6±1	56.5±1
Mass (kg)	19.6±0.5	25.0±2
SEA (kJ/kg)	2.89±0.1	2.26±0.1

Fig. 10 T-direction force-displacement curves and results (average of test data for 3 specimens in each case)

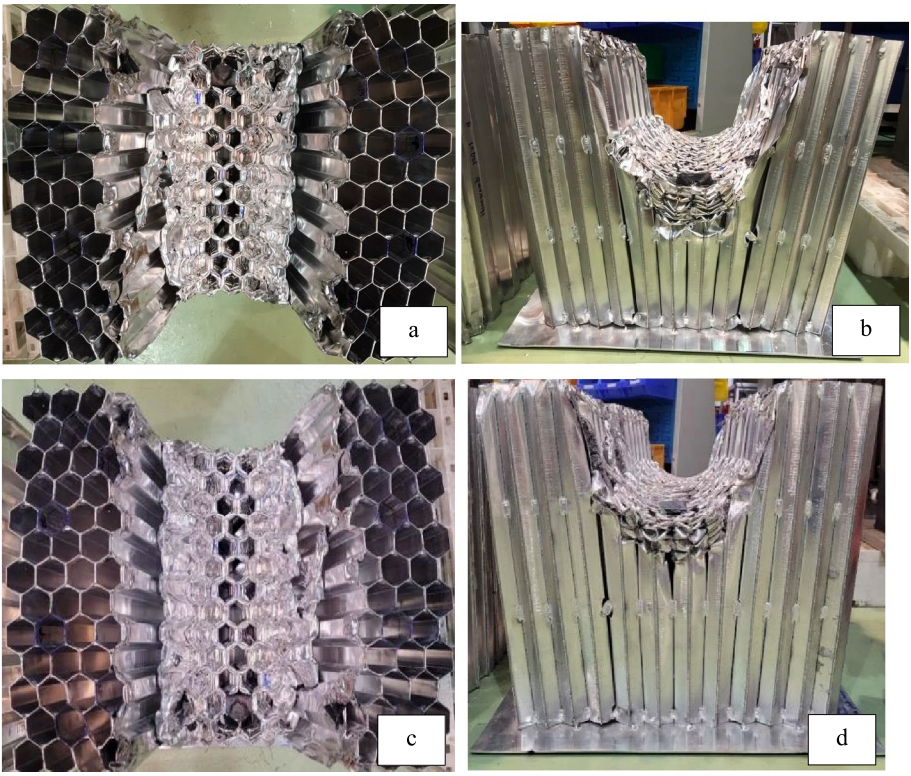

Fig. 11 **a**, **c** Top view and **b**, **d** side view of the empty and foam-filled specimens, respectively, after T-direction impact tests

is greater, which means that the acceleration level is also once again greater. Considering the SEA values, and only for these precise test conditions, the empty specimen is yet again more interesting from a crashworthiness perspective than the foam-filled specimen (see Fig. 13).

It can be observed that the deformation mechanism occurred through the development of folds, which started their development solely at one end of the structure. Due to the shape of the impactor, clear separations between crushed and non-crushed sheets appeared. This is due to how the sheets are assembled; four welding points are evenly dispersed along the length of the structure. In that case, the first welding point was broken between the crushed and non-crushed sheets, which resulted in a clear separation. It can be also noticed that the top of the foam fillers located at the edge of the crushed zone is dissociated from their base. Moreover, only the central part of the honeycomb was crushed, which means that the role of the foam fillers for the T-direction test was limited. This is the main reason that the foam fillers to the honeycomb structure do not improve the SEA, as the added weight through the foam is not completely engaged during the impact event (see Fig. 11).

Finally, it can be observed that the same deformation pattern as for the quasi-static test appears for the empty honeycomb structure. Concerning the foam-filled specimen, the deformation pattern is different from the quasi-static test as the L-direction test was accurately performed. The deformation pattern is in the form of two intertwined crosses which are bypassing the foam-filled cells. These patterns were also witnessed by Mozafari et al. [23] (see Fig. 13).

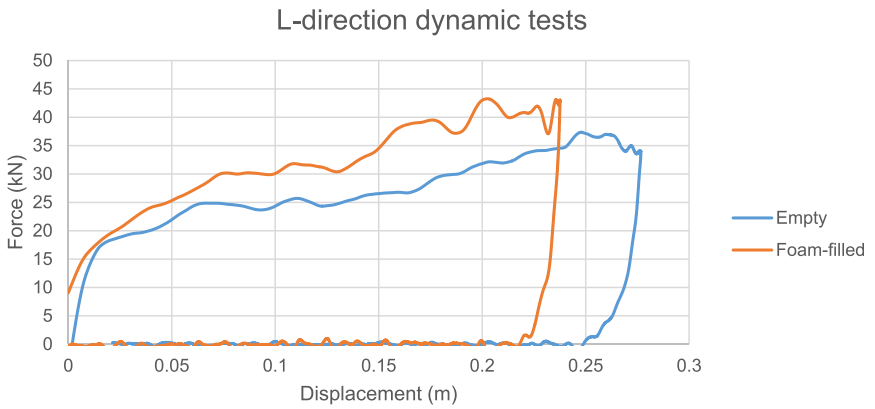

	Empty	Foam-filled
Peak force (kN)	37±2	43±2
Mean acceleration (g)	3±0.1	4±0.1
Displacement (m)	0.277±0.02	0.238±0.02
EA (kJ)	7.1±0.5	7.3±0.5
Mass (kg)	19.6±1	24.9±1
SEA (kJ/kg)	0.36±0.02	0.29±0.02

Fig. 12 L-direction force-displacement curves and results (average of test data for 3 specimens in each case)

3 Finite Element Modelling

3.1 Material Modelling

The Johnson-Cook plasticity and failure models are used to define the plasticity and, further, the failure of the material [24, 25]. The material property model can be described by

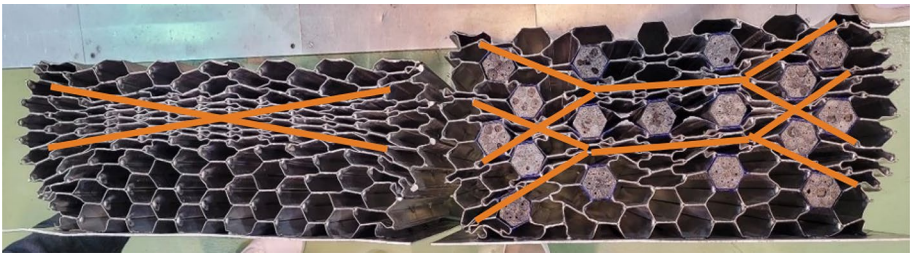

Fig. 13 Deformation pattern of the specimens after the L-direction dynamic tests, (**a**) empty and (**b**) foam-filled specimens

the Johnson-Cook model under the conditions of large deformation, high strain rate and elevated temperatures, as shown in Table 3.

Table 3 represents the parameters that define the plasticity and failure models of 1100-H14 aluminium. Parameters m, C, d_4 and d_5 were extracted from Iqbal et al. research paper [26] since parameters based on rate and temperature dependence were not experimentally tested. Regarding the aluminium foam material model, compression tests were conducted on the foam specimens made of aluminium to create a material model for use in Abaqus. The material model of stress–strain curve of the crushable foam which is incorporated into ABAQUS is shown in Fig. 14.

3.2 Foam-Filled Honeycomb Structures

The structure is composed of a honeycomb aluminium structure formed from corrugated aluminium sheets welded together, and 17 aluminium foam fillers are placed inside honeycomb cells as demonstrated in Fig. 15. The 17 aluminium fillers were optimised in the previous work of authors [21]. These dimensions were measured from the experimental tests conducted to ensure the best possible accuracy. A mass of 1500 kg was assigned to the upper plate to model the mass of a road car.

The corrugated sheets were modelled using shell elements S4R, four-node shell elements with reduced integration, hourglass control and element deletion enabled. The aluminium foam was modelled using solid element C3D8R, 3D Continuum 8-noded elements (C3D8) with reduced integration.

According to the mesh convergence analysis conducted in [21], the best compromise regarding the mesh size is to choose a mesh size of 2.5 mm for both the corrugated sheets and the foam fillers. This mesh size is therefore chosen to get the best compromise between the accuracy of results and computation time. Both the honeycomb structure and the foam fillers are fixed to the bottom plate using tie constraints, for which the master surface is the rigid plate, and the slave surfaces are the contact surfaces of the corrugated sheets and the foam filers, respectively, as shown in Figs. 16 and 17.

The tie constraint prevents any relative movement between the master and slave surfaces.

Table 3 Johnson-Cook plasticity and failure models parameters

Parameters	Values
A [MPa]	116.6
B [MPa]	32
n	0.32
T_m [C°]	775
T_r [C°]	23
m	0.86
C	0.001
ε_{ref}	1
d_1	0.075
d_2	0.33
d_3	5.34
d_4	0.147
d_5	0

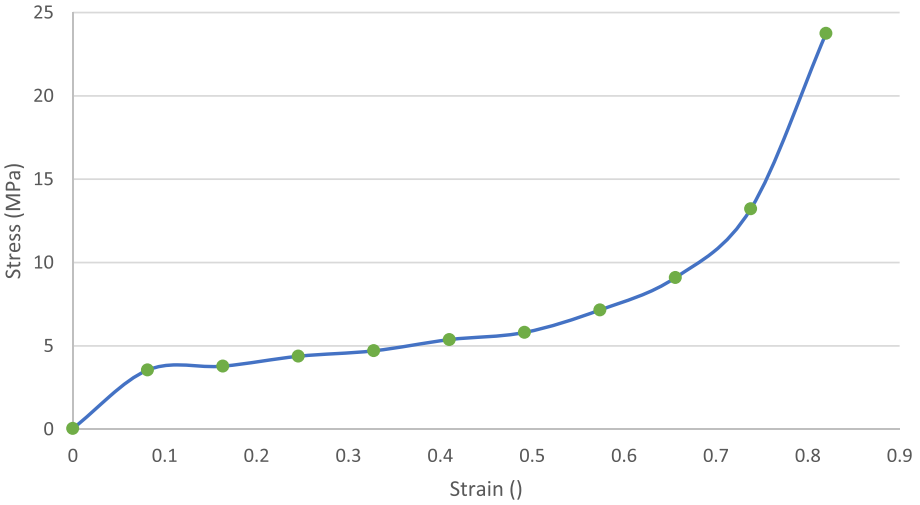

Fig. 14 Crushable foam plasticity isotropic hardening model (density: 470 kg/m^3)

A general contact is also applied to model the contact between the impactor and the structure. "Hard" contact is defined as the normal behaviour to prevent the impactor from penetrating the structure, and a tangential behaviour with a friction coefficient value of 0.2 is also created to model the interaction between the foam fillers and the honeycomb cells [21, 22, 24]. The comparison between experimental and numerical results in both T and L directions are shown in Figs. 18 and 19.

Two boundary conditions are used for these models. The first boundary condition concerns the lower plate, which is built-in, meaning that all displacements and rotations are prevented. The structure is fixed to a wall during a dynamic impact test at the CIC or would be fixed to the road service vehicle during a crash scenario. The second boundary condition concerns the upper plate, or impactor, which is only allowed to move along the axial

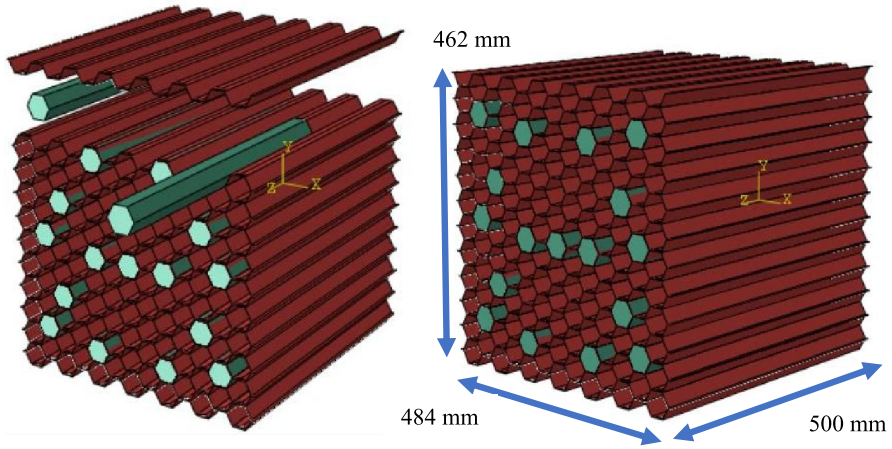

Fig. 15 The geometry of the foam-filled honeycomb model

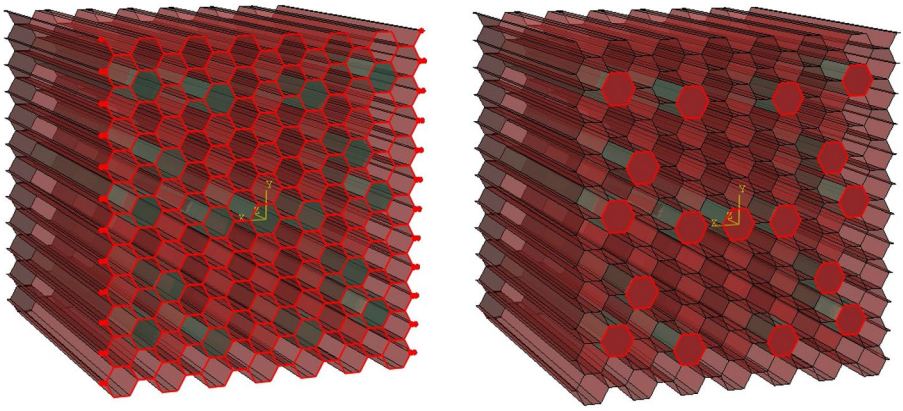

Fig. 16 Representation of the contact surfaces of the honeycomb structure and foam fillers with the lower plate

(Z) direction at a fixed velocity of 20 m/s. This is supposed to simulate the displacement of a road vehicle impacting the safety vehicle and the honeycomb structure.

3.3 Reinforced Honeycomb Structure

As a result, in Sect. 3.2, it is necessary to find ways to increase the force levels of the structure, so that the specimen can absorb all the impactor energy without reaching the densification zone leading to excessive force levels.

As referred in [6], compared to the traditional regular hexagonal honeycomb, the reinforced regular hexagonal honeycomb would improve the energy absorption capability under the same limit of peak stress. This statement is based on axial impact tests, but it is worth considering under L-direction impact as well. Then, one can vary the thickness of the stiffeners to adjust the force to the desired level. Stiffeners in the form of aluminium plates are added between each corrugated sheet of the honeycomb structure. At first, the thickness of the stiffeners can be set at 1 mm, like the thickness of the corrugated sheets. Variable thicknesses will be set to test the influence on the force levels. The model of the reinforced honeycomb structure is presented in Fig. 20. According to previous work of authors presented in [21], when looking at the effect of

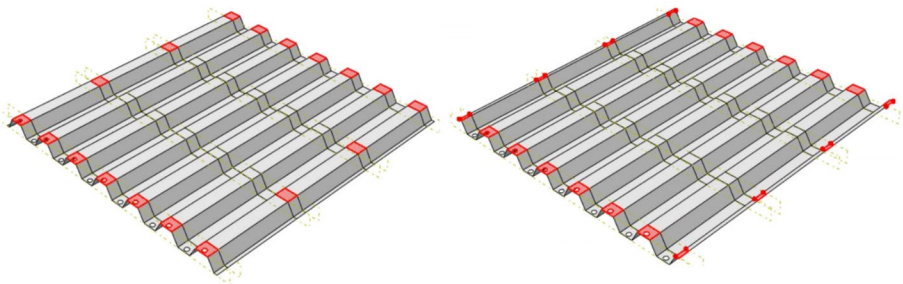

Fig. 17 Upper and lower surfaces of the tie constraint involving the corrugated sheets

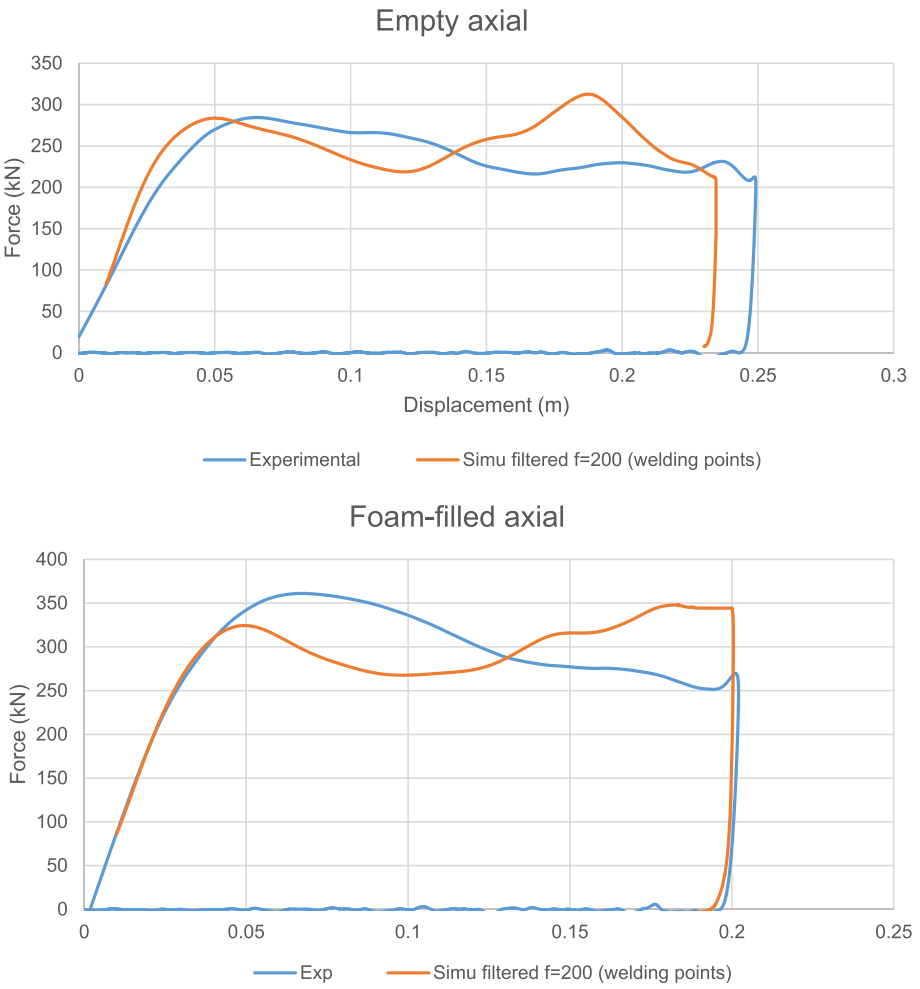

Fig. 18 Comparison between the experimental and the numerical results for the foam-filled specimen in T and L directions

the foam fillers on the force levels under L-direction impact, it has been concluded that their presence is not useful from a crashworthiness behaviour's point of view. The SEA value is better for the empty specimen.

The results of the numerical simulation under road conditions are given in Fig. 20. It is shown that the initial force level consequently increased compared to the regular honeycomb structure's results. The force level is around 150 kN whereas it was around 30 kN for the regular structure. However, the structure is still not stiff enough to avoid the total collapse of the structure and the entry into the densification zone, leading to extreme force levels (see Fig. 21). It is then worth discovering if an increase in the stiffener's thickness will cope with this problem.

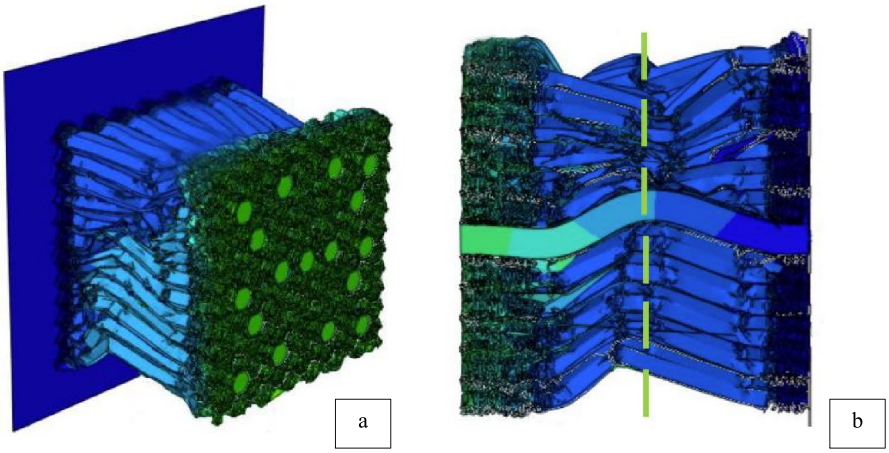

Fig. 19 **a** Initial and **b** end state of the impact test in the T-direction

3.4 Influence of the Stiffener Thickness

The thickness of the stiffener is increased from 1 to 3 mm, to observe the influence on the mean crushing force. One can easily deduce that the stiffener's thickness hardly influences the mean crushing force. Indeed, due to increase of wall thickness from 1 to 3 mm, the mean crushing force increased from 129 kN to 148 kN. This growth is not

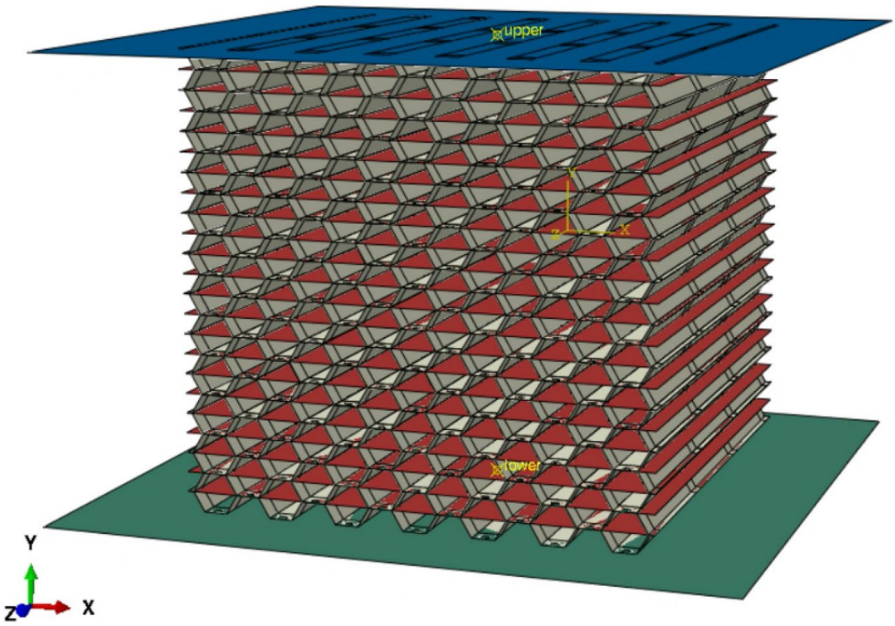

Fig. 20 Model of the reinforced honeycomb structure

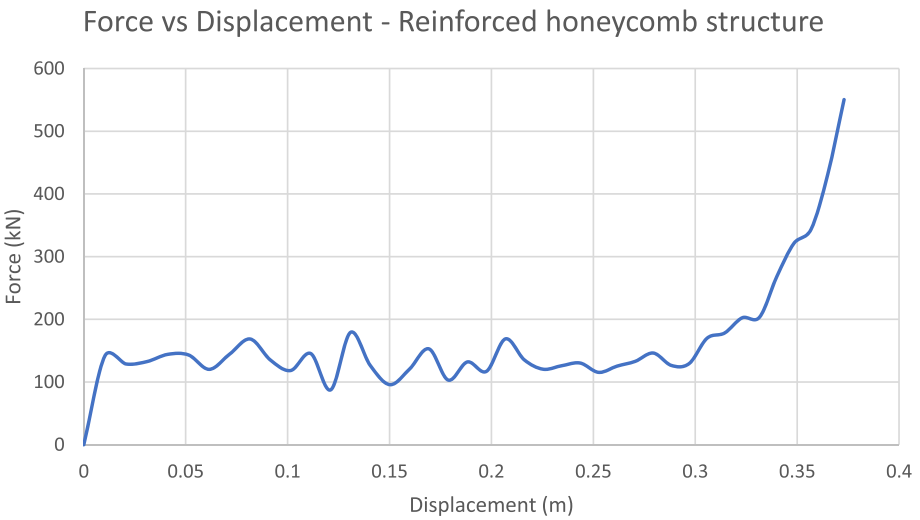

Fig. 21 The force-displacement curve of the L-direction impact on the reinforced structure under road (real) conditions

at all sufficient as the goal is to obtain a mean crushing force of 300 kN. Thickening the stiffeners would lead to a loss of efficiency of the structure, as the small increase in mean force would not make up for the gain in mass (see Fig. 22).

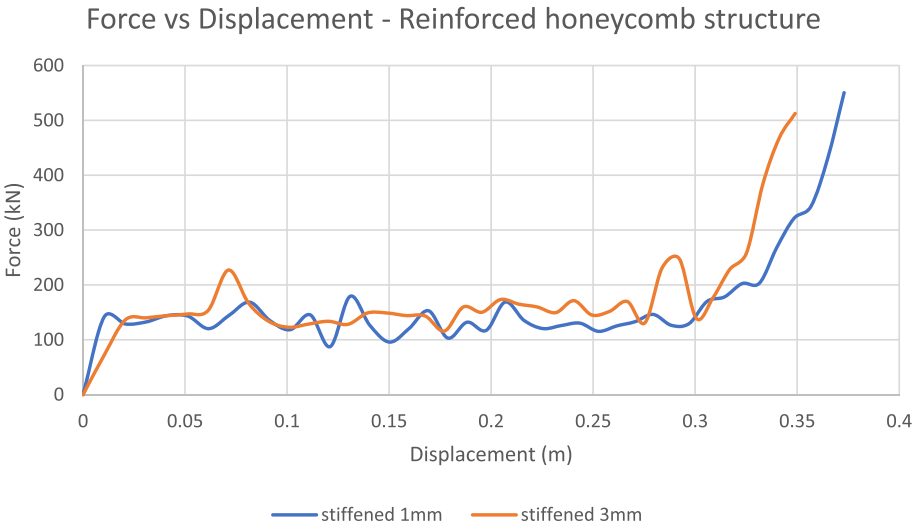

Fig. 22 Influence of the stiffener's thickness on the force-displacement curve

4 Conclusions

Experimental tests were performed and allowed witnessing and understanding of the actual crashworthiness behaviour of the different specimens tested. Both the empty and foam-filled honeycomb specimens were tested statically and dynamically, in two different impact directions.

For T-direction, it was noticed that the top of the foam fillers located at the edge of the crushed zone is dissociated from their base while the central part of the honeycomb was crushed, which means that the role of the foam fillers for the T-direction test was limited. This is the main reason that the foam fillers to the honeycomb structure do not improve the SEA, as the added weight through the foam is not completely engaged during the impact event.

For L-direction, it was concluded that the same deformation pattern as for the quasi-static test appears for the empty honeycomb structure. Concerning the foam-filled specimen, the deformation pattern is different from the quasi-static test. The deformation pattern was in the form of two intertwined crosses which bypass the foam-filled cells. Due to increase of wall thickness from 1 to 3 mm, the mean crushing force increased from 129 kN to 148 kN. This growth is not sufficient as the goal is to obtain a mean crushing force of 300 kN. Thickening the stiffeners would lead to a loss of efficiency of the structure, as the small increase in mean force would not make up for the gain in mass.

Using the material models from both the previous work [7] and the new foam compression tests conducted at the Thailand National Metal and Materials Technology Centre, the FE models were developed in ABAQUS. Exploiting the force-displacement tests from both the experimental tests and the simulations, as well as comparing the main crashworthiness parameters, allowed us to confidently validate the FE models.

Once the FE models were validated, changes were made to the geometry to improve the crashworthiness behaviour of the structure under an impact at a speed of 50 km/h and a mass of 1500 kg and ensure the maximum deceleration level is not exceeded. The impact load was conducted on the structure in the L-direction. It has been shown that to get a crash box matching the energy absorption and deceleration requirements under that impact direction, it is, therefore, necessary to reinforce it by using stiffeners. It has also been proven that the thickness of these stiffeners will not significantly influence the force levels. Thus, increasing the corrugated sheet' thickness becomes necessary. The main shortcoming of this research would be related to the effect of stiffener geometry and thickness which showed a minor contribution to the energy absorption capability of the honeycomb structures. This design should be studied further to introduce an optimised geometry such auxetic cores to improve energy efficiency without weight penalty.

Author Contributions G. Nicoud: Investigation, Formal analysis, Writing - Original Draft. H. Ghasemnejad: Conceptualization, Methodology, Supervision, Writing – Review and Editing. S. Srimanosaowapak: Conceptualization, Methodology, Supervision, Writing – Review and Editing. J.W. Watson: Conceptualization, Methodology, Supervision.

Funding This research was carried out in collaboration with the industry partner, Thailand Metal and Materials Technology Center (MTEC) and Bangkok Expressway and Metro Public Company Ltd. This work was also sponsored by the Royal Academy of Engineering (RAE) through the Engineering X Transforming Systems through Partnership programme. All funding resources are acknowledged.

Data Availability The datasets generated during and/or analysed during the current study are available from the corresponding author on reasonable request.

Declarations

Consent for Publication Submission of this article implies that the work described has not been published previously, that it is not under consideration for publication elsewhere.

Conflict of Interest The authors declare no conflict of interest.

References

1. Partovi Meran, A., Toprak, T., Muğan, A.: Numerical and experimental study of crashworthiness parameters of honeycomb structures. Thin-Walled Struct. **78**, 87–94 (2014). https://doi.org/10.1016/j.tws.2013.12.012
2. Yin, H., Wen, G.: Theoretical prediction and numerical simulation of honeycomb structures with various cell specifications under axial loading. Int. J. Mech. Mater. Des. **7**(4), 253–263 (2011). https://doi.org/10.1007/s10999-011-9163-5
3. Garai, F., Béres, G., Weltsch, Z.: Development of tubes filled with aluminium foams for lightweight vehicle manufacturing. Mater. Sci. Eng. A. 790 (2020). https://doi.org/10.1016/j.msea.2020.139743
4. Dipen Kumar Rajak, Nikhil, N., Mahajan: Emanoil Linul crashworthiness performance and microstructural characteristics of foam-filled thin-walled tubes under diverse strain rate. J. Alloys Compd. **775**, 675–689 (2019)
5. Hsu, S.S., Jones, N.: Quasi-static and dynamic axial crushing of circular and square stainless steel tubes. Int. J. Crashworthiness **9**, 195–217 (2002)
6. He, Q., Ma, D.W.: Parametric study and multi-objective crashworthiness optimisation of reinforced hexagonal honeycomb under dynamic loadings. Int J Crashworthiness **20**(5), 495–509 (2015). https://doi.org/10.1080/13588265.2015.1041324
7. Abd El-baky, M.A., Hegazy, D.A., Hassan, M.A., Kamel, M.: Potentiality of halloysite nanoclay on crashworthiness performance of polymer composite tubular elements. J. Compos. Mater. **56**(12), 1901–1919 (2022). https://doi.org/10.1177/00219983221088099
8. Alshahrani, H., Sebaey, T.A., Hegazy, D.A.: M. A. Abd El-baky. Development of efficient energy absorption components for crashworthiness applications: An experimental study. Polym. Adv. Technol. **33**, 2921–2942 (2022). https://doi.org/10.1002/pat.5759
9. Abd El-baky, M.A., Hegazy, D.A., Hassan, M.A.: Novel energy absorbent composites for crashworthiness applications. **51**(4), 6403S-6442S (2022). https://doi.org/10.1177/15280837221086040
10. Awd Allah, M.M., Shaker, A., Hassan, M.A.: M.A. Abd El-baky, the influence of induced holes on crashworthy ability of glass reinforced epoxy square tubes. Polym. Compos. **43**, 8322–8340. https://doi.org/10.1002/pc.27004
11. Abd El-baky, M.A., Hegazy, D.A., Hassan, M.A.: Advanced Thin-walled composite structures for energy absorption applications. Appl. Compos. Mater. **29**, 1195–1233 (2022). https://doi.org/10.1007/s10443-022-10016-5
12. Alshahrani, H., Sebaey, T.A., Awd Allah, M.M.: and M.A. Abd El-baky, multi-response optimization of crashworthy performance of perforated thin walled tubes. J. Compos. Mater. **57**(9), 1579–1597. https://doi.org/10.1177/00219983231159508
13. Yu, J., Shi, Z., Dong, X., Li, Q., Lv, J., Ren, Z.: Impact Time Consensus Cooperative Guidance against the Manoeuvring Target: Theory and experiment. IEEE Trans Aerosp Electron Syst **59**(4), 4590–4603 (2023). https://doi.org/10.1109/TAES.2023.3243154
14. Tian, L., Li, M., Li, L., Li, D., Bai, C.: Novel joint for improving the collapse resistance of steel frame structures in column-loss scenarios. Thin-Walled Struct. **182**, 110219 (2023)

15. Wang, Y., Lou, M., Wang, Y., Wu, W., Yang, F.: Stochastic failure analysis of Reinforced Thermoplastic pipes under Axial Loading and Internal pressure. China Ocean. Eng. **36**(4), 614–628 (2022). https://doi.org/10.1007/s13344-022-0054-3
16. Zhang, C., Khorshidi, H., Najafi, E., Ghasemi, M.: Fresh, mechanical and microstructural properties of alkali-activated composites incorporating nanomaterials: A comprehensive review. J Clean Prod **384**, 135390 (2023)
17. Zhang, W., Kang, S., Liu, X., Lin, B., Huang, Y.: Experimental study of a composite beam externally bonded with a carbon fiber-reinforced plastic plate. J. Building Eng. **71**, 106522 (2023)
18. Guo, H., Zhang, J.: Expansion of Sandwich Tubes with Metal Foam Core under Axial Compression. J Appl Mech **90**(5), 051008 (2023). https://doi.org/10.1115/1.4056686
19. Yu, H., Zhang, J., Fang, M., Ma, T., Wang, B., Zhang, Z., Yang, K.: Bio-inspired strip-shaped composite composed of glass fabric and waste selvedge from A. Pernyi silk for lightweight and high-impact applications. Compos Part A: Appl Sci Manufac **174**, 107715 (2023)
20. Duarte, A.P.C., Mazzuca, P., Lopo de Carvalho, J.M., Tiago, C., Firmo, J.P., Correia, J.R.: Determination of the temperature-dependent thermophysical properties of polymeric foams using numerical inverse analysis. **394**(29), 131980 (2023)
21. Silva, G.: Development of Aluminium Foam Crash Box for Crashworthiness Performance. MSc Thesis, Cranfield University. (2021)
22. ISO:, Mechanical testing of metals - Ductility Testing - Compression test for porous and cellular metalsInt. Stand **ISO 13314**(1) (2011)
23. Mozafari, H., Khatami, S., Molatefi, H., Crupi, V., Epasto, G., Guglielmino, E.: Finite element analysis of foam-filled honeycomb structures under impact loading and crashworthiness design. Int J Crashworthiness **21**(2), 148–160 (2016). https://doi.org/10.1080/13588265.2016.1140710
24. Zarei, H., Kröger, M.: Optimum honeycomb filled Crash absorber design. Mater Des **29**(1), 193–204 (2008). https://doi.org/10.1016/j.matdes.2006.10.013
25. Johnson, G.R., Cook, W.H.: Fracture characteristics of three metals subjected to various strains, strain rates, temperatures and pressures. Eng. Fract. Mech. **21**(1), 31–48 (1985). https://doi.org/10.1016/0013-7944(85)90052-9
26. Iqbal, M.A., Khan, S.H., Ansari, R., Gupta, N.K.: Experimental and numerical studies of double-nosed projectile impact on aluminium plates. Int. J. Impact Eng. **54**, 232–245 (2013). https://doi.org/10.1016/j.ijimpeng.2012.11.007